High-Throughput Screening To Identify Inhibitors Which Stabilize Inactive Kinase Conformations in p38α

ARTICLE *in* JOURNAL OF THE AMERICAN CHEMICAL SOCIETY · DECEMBER 2009

Impact Factor: 12.11 · DOI: 10.1021/ja907795q · Source: PubMed

11 AUTHORS, INCLUDING:

Jeffrey R Simard
Amgen
41 PUBLICATIONS **1,299** CITATIONS
SEE PROFILE

Vijaykumar Pawar
Florentis Pharmaceuticals Pvt. Ltd.
20 PUBLICATIONS **362** CITATIONS
SEE PROFILE

Alexander Wolf
Lead Discovery Center
22 PUBLICATIONS **423** CITATIONS
SEE PROFILE

Christian Ottmann
Technische Universiteit Eindhoven
82 PUBLICATIONS **1,376** CITATIONS
SEE PROFILE

J|A|C|S
ARTICLES

High-Throughput Screening To Identify Inhibitors Which Stabilize Inactive Kinase Conformations in p38α

Jeffrey R. Simard, Christian Grütter, Vijaykumar Pawar, Beate Aust, Alexander Wolf, Matthias Rabiller, Sabine Wulfert, Armin Robubi, Sabine Klüter, Christian Ottmann, and Daniel Rauh*

Chemical Genomics Centre of the Max Planck Society, Otto-Hahn-Strasse 15, D-44227 Dortmund, Germany

Received September 22, 2009; E-mail: daniel.rauh@cgc.mpg.de

Abstract: Small molecule kinase inhibitors are an attractive means to modulate kinase activities in medicinal chemistry and chemical biology research. In the physiological setting of a cell, kinase function is orchestrated by a plethora of regulatory processes involving the structural transition of kinases between inactive and enzymatically competent conformations and *vice versa*. The development of novel kinase inhibitors is mainly fostered by high-throughput screening initiatives where the small molecule perturbation of the phosphorylation reaction is measured to identify inhibitors. Such setups require enzymatically active kinase preparations and present a risk of solely identifying classical ATP-competitive Type I inhibitors. Here we report the high-throughput screening of a library of ~35000 small organic molecules with an assay system that utilizes enzymatically inactive human p38α MAP kinase to detect stabilizers of the pharmacologically more desirable DFG-out conformation. We used protein X-ray crystallography to characterize the binding mode of hit compounds and reveal structural features which explain how these ligands stabilize and/or induce the DFG-out conformation. Lastly, we show that although some of the hit compounds were confirmed by protein X-ray crystallography, they were not detected in classic phosphorylation assays, thus validating the unique sensitivity of the assay system used in this study and highlighting the potential of screening with inactive kinase preparations.

1. Introduction

Aberrantly regulated kinases play causative roles in a wide range of human disorders and particularly in the onset of several types of cancer. Despite recent advances in targeted tumor therapy, lack of inhibitor selectivity and efficacy, drug target validation and the emergence of kinase drug resistance remain key challenges.[1] To overcome these limitations, current medicinal chemistry efforts aim to develop kinase inhibitors such as the well-known anticancer drug imatinib (Gleevec), which target inactive or DFG-out kinase conformations.[2,3] Gleevec is an example of a Type II inhibitor which binds partially within the ATP binding site while also extending into an allosteric binding pocket and stabilizes the inactive kinase conformation. Type III inhibitors also stabilize the DFG-out conformation but bind exclusively within the allosteric pocket. The structural transition associated with the binding of both Type II or Type III inhibitors increases the drug−target residence time and increases efficacy at lower drug concentrations, thereby augmenting the therapeutic window.[4]

Classical kinase inhibitors (Type I), such as staurosporine, bind exclusively within the ATP binding site of the active DFG-in kinase conformation in which the activation loop is open and extended such that ATP and substrate molecules can bind. However, the amino acids lining the ATP binding pocket are highly conserved by nature, making the design of specific Type I inhibitors particularly challenging. Considering that the amino acids lining the allosteric pocket are much less conserved, one would expect methods for identifying ligands which bind to inactive kinase conformations (Type II/III inhibitors) to be a valuable commodity for guiding innovative compound design. Until recently, approaches that allow for the unambiguous identification of such inhibitors have fallen short and are incompatible for high-throughput screening (HTS).[5,6] Using the newly developed FLiK (fluorescent labels in kinases) assay system in which kinases of interest are specifically labeled on the activation loop with the environmentally sensitive fluorophore acrylodan,[7,8] we recently identified compounds that served as excellent starting points for the design and synthesis of potent

(1) Zhang, J.; Yang, P. L.; Gray, N. S. *Nat Rev Cancer* **2009**, *9*, 28–39.
(2) Backes, A. C.; Zech, B.; Felber, B.; Klebl, B.; Müller, G. *Expert Opin Drug Discovery* **2008**, *3*, 1409–1425.
(3) Backes, A. C.; Zech, B.; Felber, B.; Klebl, B.; Müller, G. *Expert Opin Drug Discovery* **2008**, *3*, 1427–1449.
(4) Copeland, R. A.; Pompliano, D. L.; Meek, T. D. *Nat Rev Drug Discov* **2006**, *5*, 730–9.
(5) Annis, D. A.; Nazef, N.; Chuang, C. C.; Scott, M. P.; Nash, H. M. *J. Am. Chem. Soc.* **2004**, *126*, 15495–503.
(6) Vogtherr, M.; Saxena, K.; Hoelder, S.; Grimme, S.; Betz, M.; Schieborr, U.; Pescatore, B.; Robin, M.; Delarbre, L.; Langer, T.; Wendt, K. U.; Schwalbe, H. *Angew. Chem., Int. Ed. Engl.* **2006**, *45*, 993–7.
(7) Simard, J. R.; Getlik, M.; Grutter, C.; Pawar, V.; Wulfert, S.; Rabiller, M.; Rauh, D. *J. Am. Chem. Soc.* **2009**, *131*, 13286–13296.
(8) Simard, J. R.; Kluter, S.; Grutter, C.; Getlik, M.; Rabiller, M.; Rode, H. B.; Rauh, D. *Nat Chem Biol* **2009**, *5*, 394–396.

Type II inhibitors which are able to overcome mutation-associated drug resistance in the tyrosine kinase cSrc.[9]

Here we report the use of this assay in a high-throughput format. We screened a library of ~35000 compounds and identified 26 which bind to and stabilize the inactive kinase conformation of human p38α MAP kinase. Since initial screening for these compounds used the inactive (i.e., unphosphorylated) form of the kinase, hit validation and enzyme inhibition were verified using an activity-based kinase assay. Surprisingly, in addition to DFG-out binding Type II and Type III inhibitors, several Type I inhibitors which stabilize the inactive kinase conformation were also identified. We utilized protein X-ray crystallography to identify several interesting structural features which explain how some of these Type I ligands may stabilize and/or induce the DFG-out conformation. We also used protein X-ray crystallography to identify the first reported DFG-out binding thiazole-urea compounds and reveal a new Type III binding mode for this scaffold, thus highlighting the impact which our novel assay system may have on future medicinal chemistry endeavors in the field of kinase research.

2. Materials and Methods

2.1. Materials. The fluorophore 6-acryloyl-2-dimethylaminonaphthalene (acrylodan) was purchased from Invitrogen GmbH (Karlsruhe, Germany). Crystallization plates (EasyXtal Tool; 24-well) were obtained from Qiagen GmbH (Hilden, Germany). Cuvettes and mini stir bars were obtained from Carl Roth GmbH (Karlsruhe, Germany). Small volume (20 μL fill volume) black flat bottom 384-well plates were obtained from Greiner Bio-One GmbH (Solingen, Germany). All supplies for the p38α HTRF assay kit were purchased from CisBio (Bagnols-sur-Cèze, France). Additional compounds for SAR studies were purchased from ChemDiv (San Diego, CA). Thiazole-urea compounds identified as DFG-out binders in our screen were part of a commercially available 602 compound library from BioFocus DPI (Saffron Walden, UK) designed and predicted to be potential DFG-out binders using the docking software FLEX-X.

2.2. Protein Expression, Purification, Labeling, and Activation. Nonphosphorylated (inactive) human p38α MAP kinase was expressed, purified, and labeled as described previously.[7] Briefly, an N-terminal His-p38α construct containing the mutations required for specific labeling of the activation loop (C119S/C162S/A172C), as well as wild type p38α, were transformed into BL21(DE3) *E. coli*, overexpressed at 18 °C and purified by Ni-affinity, anion exchange, and size exclusion chromatography as described previously. The pure unphosphorylated protein was subsequently concentrated to ~10 mg/mL and used for fluorescence labeling.

For IC_{50} measurements, small amounts of constitutively active MKK6 (S207E/T211E) (obtained from Invitrogen; Carlsbad, CA) were used to activate wild type p38α (see section 2.5 for details). For K_d determinations using phosphorylated active p38α, a larger amount of constitutively active MBP-tagged MKK6 (S207D/T211D) was first expressed using a construct obtained from the University of Dundee. The p38α construct (C119S/C162S/A172C) designed for the FLiK assay was then activated using a protocol described elsewhere[10] and subsequently labeled with acrylodan as previously described.[7] Phosphorylation and labeling were confirmed using ESI-MS also as described previously.[7]

2.3. High-Throughput Screen of a Large Compound Library. A primary screen was carried out using a single concentration (12.5 μM) of each library compound to first determine which compounds induce and stabilize the DFG-out conformation of p38α. Inhibitor predilution plates were prepared by diluting compounds from the stock plates (1 compound per well at 10 mM in DMSO) to 50 μM in buffer (50 mM Hepes pH 7.45, 200 mM NaCl, 0.01% Triton-X100). Large volumes of the same buffer were also used to prepare the solutions for pipetting both screening plates (+133.3 nM acrylodan-labeled p38α) and background plates (no labeled kinase added). A Freedom EVO pipetting Robot (programmed with the Freedom EVOware Plus software from Tecan), equipped with an eight channel liquid-handling arm with a low volume option and a 384-channel TeMo head, was used to first dispense 5 μL of prediluted compounds into a set of two 384-well small volume assay plates. Subsequently, 15 μL of buffer were added to the background plate, while the same volume of buffer containing the labeled kinase was added to the screening plate to detect DFG-out binders. The final concentration of acrylodan-labeled p38α was 100 nM, and the %v/v DMSO was <0.2%. All plates also contained 6 wells of negative DMSO control (no ligand) as well as 6 wells of positive control (12.5 μM BIRB-796). Both plates were covered with adhesive foil and stored at 4 °C overnight since DFG-out binders are known to have very slow association rates in p38α.[11]

A Tecan Safire^2 instrument was used to measure the fluorescence readout in the 384-well plate format. Data were first processed by subtracting intrinsic compound fluorescence at 514 and 468 nm from the signal intensity (I) measured in the presence of acrylodan-labeled p38α. As described previously, the extent of binding was then assessed by taking the corrected ratiometric fluorescence ($R = I_{\lambda 514}/I_{\lambda 468}$).[7] Any compound which reached 25% of the maximal response observed for the positive control was submitted for further screening. All subsequent data management and screening data analysis were performed with the software AccordHTS and Pipeline Pilot from Accelrys.

The secondary screen was also carried out in 384-well plates using a range of concentrations of each ligand (100 nM to 50 μM) to generate binding curves or identify false hits which were picked up due to high intrinsic fluorescence which was not adequately subtracted by using background plates. Predilution plates were prepared using buffer such that the compound concentration was 2-fold higher than that needed in the final screening plate. The robot first dispensed 3.5 μL of the prediluted compounds into a set of 384-well small volume assay plates. Each plate contained no more than 7 different compounds, each screened at 10 concentrations and 4 wells per concentration. Subsequently, 3.5 μL of buffer were added to the background plate, while the same volume of buffer containing the 200 nM labeled kinase was added to the screening plate to give a final concentration of 100 nM acrylodan-labeled p38α. Plates were sealed, incubated, and measured as described for the primary screen. Raw data at 514 and 468 nm as well as background-corrected ratiometric data were used to eliminate false fluorescent hits. Ratiometric fluorescence values enabled binding curves to be plotted to directly determine the K_d of ligand binding to p38α. Where indicated, binding curves were plotted as % p38α bound by the ligand and was calculated as follows:

$$\%\ \text{p38}\alpha\ \text{bound} = (R - R_{\text{unsat}})/(R_{\text{sat}} - R_{\text{unsat}}) \times 100$$

where R is the ratiometric fluorescence at a given concentration of ligand and R_{unsat} and R_{sat} are the ratiometric fluorescence values obtained for p38α in the absence or presence of a saturating concentration of the same ligand, respectively. All compounds yielding a sigmoidal binding curve were then subjected to LC-MS analysis to assess purity and to confirm their correct molecular masses.

(9) Getlik, M.; Grutter, C.; Simard, J. R.; Kluter, S.; Rabiller, M.; Rode, H. B.; Robubi, A.; Rauh, D. *J. Med. Chem.* **2009**, *52*, 3915–26.

(10) Sullivan, J. E.; Holdgate, G. A.; Campbell, D.; Timms, D.; Gerhardt, S.; Breed, J.; Breeze, A. L.; Bermingham, A.; Pauptit, R. A.; Norman, R. A.; Embrey, K. J.; Read, J.; VanScyoc, W. S.; Ward, W. H. *Biochemistry* **2005**, *44*, 16475–90.

(11) Pargellis, C.; Tong, L.; Churchill, L.; Cirillo, P. F.; Gilmore, T.; Graham, A. G.; Grob, P. M.; Hickey, E. R.; Moss, N.; Pav, S.; Regan, J. *Nat. Struct. Biol.* **2002**, *9*, 268–72.

2.4. LC-MS Analysis of Hit Compounds. Mass measurements and the purity of all hit compounds were determined by LC-MS analysis using an HPLC system from Agilent (1200 series) equipped with an Eclipse XDB-C18, 5 μm column (column dimensions: 150 mm × 4.60 mm) from Agilent, UV detection at 254 nm and coupled to a Thermo Finnigan LCQ Advantage Max ESI-Spectrometer. H_2O with 0.1% formic acid (solvent A) and acetonitrile with 0.1% formic acid (solvent B) were used at a flow rate of 1 mL/min. Gradient: (0 min) 90% solvent A/10% solvent B; (1 min) 90% solvent A/10% solvent B; (10 min) 0% solvent A/100% solvent B; (12 min) 0% solvent A/100% solvent B; (15 min) 90% solvent A/10% solvent B.

2.5. IC_{50} Determination with an in Vitro Activity Based Assay. To first activate p38α for IC_{50} measurements, 600 ng of active MKK6 (S207E/T211E) (obtained from Invitrogen; Carlsbad, CA) were diluted in 25 μL of 50 mM Tris-HCl, pH 7.5 supplemented with 0.1 mM EGTA, 0.1 mM sodium orthovanadate, and 0.1% v/v β-mercaptoethanol. Approximately 7 μg of inactive p38α were then added, and the solution was supplemented with 100 μM ATP and 10 mM $MgCl_2$ prior to incubation for 90 min at 37 °C with constant agitation. ATP was subsequently removed by overnight dialysis (25 mM Tris pH 8.0, 150 mM NaCl and 10% v/v glycerol) prior to IC_{50} determinations with the HTRF (homogeneous time-resolved fluorescence) assay from Cisbio according to manufacturer's instructions and as described previously,[7] using ATF2 as the substrate together with anti-ATF2 and anti-GST antibodies for detection.

2.6. Real-Time Kinetics To Predict Ligand Binding Mode. Kinetics of the association of various hits were determined using cuvettes as described previously.[7] A mini stir bar was placed in the bottom of each cuvette to ensure rapid mixing as inhibitor was delivered through the injection port located above the cuvette. Fluorescence changes were monitored at 468 nm in real-time using a JASCO FP-6500 fluorescence spectrophotometer (JASCO GmbH, Groβ-Umstadt, Germany). Near instantaneous binding kinetics (<5 s) are characteristic of Type I inhibitors while slower kinetics (>10 s) clearly indicate the slow binding of Type II or Type III inhibitors to the DFG-out conformation, in the case of p38α.[7]

It should be noted that binding modes of hit molecules can also be assessed in HTS formats by measuring plates from primary and/or secondary screens at different time points. Compounds that further reduce the fluorescence signal over time have a slow binding kinetic and are likely to be Type II/III inhibitors.

2.7. Protein Crystallography. Various inhibitors were cocrystallized with unphosphorylated p38α using conditions similar to those previously reported for unmodified p38α.[7,12] Briefly, protein−inhibitor complexes were prepared by mixing 40 μL of p38α (10 mg/mL) with 0.4 μL of inhibitor (300 mM in DMSO) and incubating the mixture for 1−2 h on ice. Samples were centrifuged at 13000 rpm for 5 min to remove excess inhibitor. In some cases, cocrystallization carried out in the presence of excess inhibitor improved the occupancy of the compounds in the crystal structure. Crystals were grown in 24-well crystallization plates using the hanging drop vapor diffusion method and by mixing 1.5 μL of protein−inhibitor solution with 0.5 μL of reservoir (100 mM MES pH 5.6−6.2, 20−30% PEG4000 and 50 mM *n*-octyl-β-D-glucopyranoside).

3. Results

3.1. HTS Screen Summary. Using our acrylodan-labeled kinase binding assay,[7,8] we screened a large collection of compound libraries against p38α labeled on the activation loop to identify ligands which specifically bind to and stabilize the inactive DFG-out conformation (Figure 1). Fluorophores, such as acrylodan which are commonly used to generate fluorescent protein conjugates, are relatively small in size and sensitive to polarity and/or conformational changes. Acrylodan, in particular, is known to produce a typically robust response[13,14] and was recently shown to be highly sensitive to movements of the activation loop upon binding of DFG-out binders.[7] DFG-out binders induce a shift in the emission maximum from 468 to 514 nm which changes the ratio of the fluorescence intensities at these wavelengths ($R = I_{\lambda 514}/I_{\lambda 468}$), allowing ligand binding to be detected at equilibrium (end point measurements). Ratiometric fluorescence readouts correct for small dilution and pipetting errors between different samples within a titration series and eliminate "edge effects" which are frequently observed in small volume HTS plates.

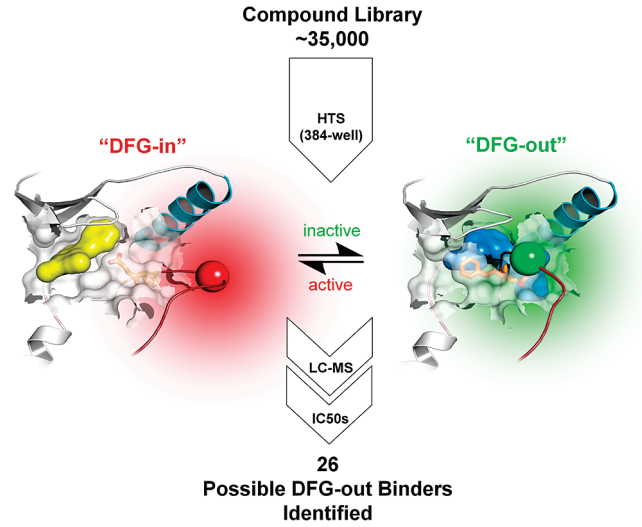

Figure 1. High-throughput screen of ~35000 compounds using the acrylodan-labeled kinase binding assay for p38α. A primary screen was carried out in 384-well small volume plates at a single concentration of each compound (12.5 μM) to identify ligands which induce the DFG-out conformation. The kinase is labeled on the activation loop with an environmentally sensitive fluorophore (colored sphere) to identify such ligands. In contrast to DFG-in binders (shown as yellow surface), DFG-out binders (shown as blue surface) induce a shift in the emission maximum from 468 to 514 nm and the dual emission maxima allow for ratiometric measurements of ligand binding to be made at equilibrium (end point measurements). These types of ratiometric fluorescence readouts are advantageous since they correct for small dilution and pipetting errors between different samples in a titration series and eliminate "edge effects" which are frequently observed due to evaporation at the edges of small volume HTS plates. All hits were then titrated against the labeled kinase in a secondary screen to determine the K_d of each potential hit. All binders were subsequently validated using small molecule LC-MS to verify the expected ligand mass and purity. Lastly, all hits were validated in an activity-based kinase inhibition assay to determine the IC_{50}. A total of 26 validated hits were identified in this screening initiative.

The complete screen was carried out by first using the labeled kinase binding assay in a 384-well HTS format to identify DFG-out binders in a library of ~35000 compounds. This was accomplished by first performing a primary screen at a single ligand concentration, followed by a secondary screen over a range of concentrations to directly determine the K_d of each potential hit. Hit validation was carried out by subjecting all confirmed hits to small molecule LC-MS analysis to assess the purity of the compound and to confirm the expected compound

(12) Bukhtiyarova, M.; Northrop, K.; Chai, X.; Casper, D.; Karpusas, M.; Springman, E. *Protein Expr Purif* **2004**, *37*, 154–61.

(13) de Lorimier, R. M.; Smith, J. J.; Dwyer, M. A.; Looger, L. L.; Sali, K. M.; Paavola, C. D.; Rizk, S. S.; Sadigov, S.; Conrad, D. W.; Loew, L.; Hellinga, H. W. *Protein Sci.* **2002**, *11*, 2655–75.

(14) Richieri, G. V.; Ogata, R. T.; Kleinfeld, A. M. *Mol. Cell. Biochem.* **1999**, *192*, 87–94.

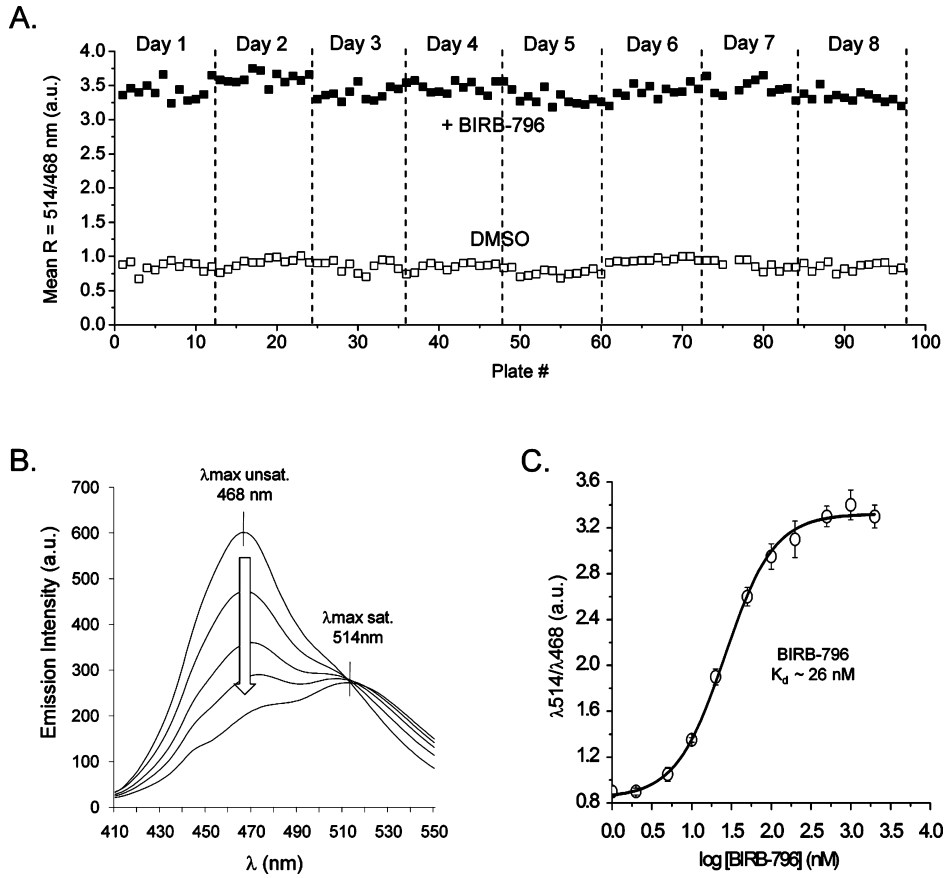

Figure 2. HTS assay performance and K_d determination of BIRB-796. Assay performance was assessed for all plates throughout the primary screen by monitoring the ratiometric fluorescence values ($R = I_{\lambda 514}/I_{\lambda 468}$) of the positive (BIRB-796) and negative (DMSO) controls and yielded a *Z*-factor of 0.82 ± 0.6 over 97 plates (A). As compounds such as BIRB-796 bind to the DFG-out conformation of p38α, there is a characteristic emission shift from 468 to 514 nm (B). Plotting the ratio of these two signals against increasing ligand concentration allows for direct determination of the K_d for BIRB-796 measured in this HTS format (C). Similar measurements were made for all screening hits. Compounds which gave sigmoidal binding curves in the secondary screen were confirmed as likely DFG-out binders while any remaining highly fluorescent compounds were easily identified as false hits. All fluorescence spectra and K_d curves shown are representative of at least three independent experiments.

mass. Follow-up validation of each hit was completed by examining inhibitory activity in a standard phosphotransfer kinase assay (HTRF). A complete overview of the HTS screen using acrylodan-labeled p38α is shown in Figure 1.

3.2. Hit Identification and Validation. A primary screen was carried out in which a single data point was obtained for each ligand (at 12.5 μM) to first determine which compounds induce and stabilize the DFG-out conformation of acrylodan-labeled p38α. Background plates were used to correct for intrinsic compound fluorescence and eliminated a large percentage of the most highly fluorescent compounds in the library. In most cases, background corrected ratiometric fluorescence values of such compounds were the same as that for the negative DMSO control (*data not shown*). The performance of the primary assay screen was assessed by monitoring the ratiometric values of the positive and negative controls of all plates and yielded a calculated *Z*-factor of 0.82 ± 0.6 for the entire screen (Figure 2a). Any compounds which reached the set cutoff (25% of the DFG-out binding positive control: BIRB-796) were then advanced to a secondary screen in which ligand binding was assessed over a concentration range of 100 nM to 50 μM. After the first round of screening, 90 compounds were identified as potential hits, corresponding to a "hit rate" of ~0.25%.

Compounds which gave sigmoidal binding curves in the secondary screen were confirmed as likely DFG-out binders, allowing highly fluorescent false hits (i.e., nonbinding compounds) to be easily identified. Changing ratiometric fluorescence values (Figure 2b) were used to plot binding curves and directly determine K_d values (Figure 2c), as shown for the positive control BIRB-796. After two rounds of screening, only 34 compounds remained likely DFG-out binders.

Before testing the hits in an activity-based assay system, all compound stocks were analyzed by LC-MS to assess the purity and to verify their expected molecular masses. Only compounds that were found to be ≥80% pure were subjected to further screening with the HTRF kinase assay for IC_{50} determinations using a wide range of inhibitor concentrations. Prior to this, each compound was initially prescreened for inhibitory activity at 50, 5, and 0.5 μM concentrations. Compounds showing minimal inhibition at 5 μM and ≥40% inhibition at 50 μM were selected for IC_{50} determinations. Following completion of these follow-up validation studies, 26 of the initial 34 hits identified as being DFG-out binders using acrylodan-labeled p38α also inhibited the enzymatic activity of p38α in the HTRF assay and were thereby validated as kinase inhibitors. The structure of several compounds (**1**−**16**), their measured K_d and IC_{50} values, and predicted binding modes are presented in Figure 3.

Compounds **3** and **5**−**9** were ultimately found to be poor inhibitors with IC_{50} values >50 μM. For all other compounds, the determined K_d and IC_{50} values were in close agreement (≤10-fold variation), thereby validating the use of a nonphosphorylated inactive acrylodan-labeled p38α for identifying DFG-

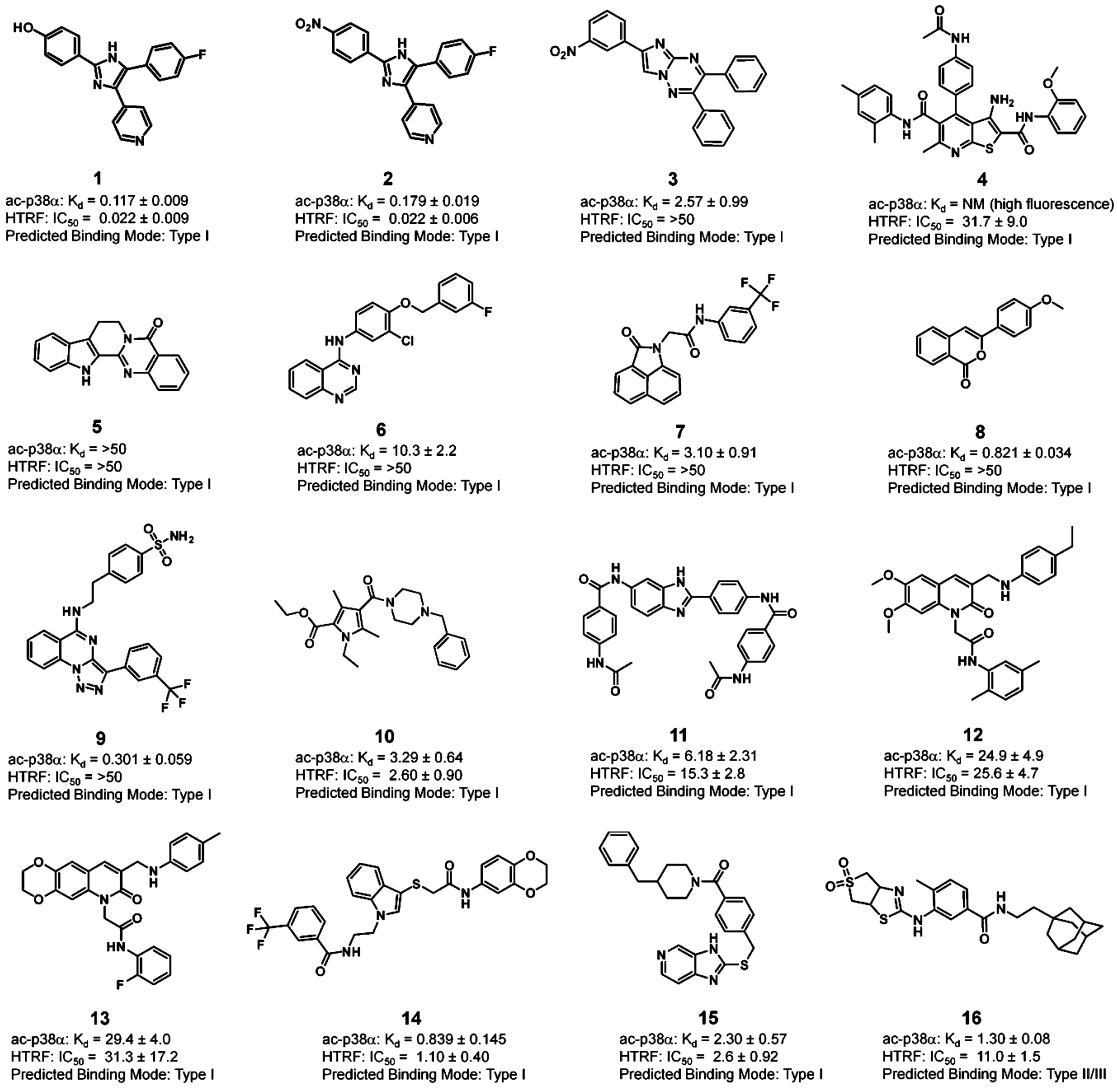

Figure 3. Chemical structures, K_d and IC_{50} values, and predicted binding modes of compounds **1**−**16**. The binding mode is assessed using real-time kinetic measurements of binding (see section 3.3). All K_d and IC_{50} values are shown in μM. K_d values were not measurable (NM) for **4**, which had high intrinsic fluorescence at high concentrations. In many cases, the K_d determined using acrylodan-labeled p38α is in close agreement with the IC_{50} values determined in activity-based assays, which validates the use of a nonphosphorylated inactive p38α for identifying DFG-out binders capable of inhibiting the active phosphorylated kinase. Some compounds are ≥20-fold less active in the activity-based assay which may be a consequence of the phosphorylation of the activation loop of p38α which is required for the activity-based HTRF assay. This likely stabilizes the DFG-in conformation of p38α. By utilizing the nonphosphorylated form of the kinase for our FLIK assay system, the DFG-out conformation is energetically more favorable and likely enhances sensitivity for the detection of DFG-out binders in large compound libraries.

out binders which have comparable activity against the active phosphorylated kinase. In the case of compounds **3** and **7**−**9**, IC_{50} values were ≥20-fold higher than the K_d values measured with our binding assay, which is larger than the variation typically observed between different assay types.

The loss of affinity for inhibitors which bind partially within the allosteric pocket adjacent to the ATP binding site is well documented when comparing the unphosphorylated kinase to the phosphorylated form of the same kinase.[15] Although not as significant as observed elsewhere for other kinases,[15] we confirmed this effect in p38α for the predicted Type II inhibitor **16** by observing a 2-fold loss of affinity when measuring the K_d using phosphorylated active acrylodan-labeled p38α (Table S1). The known Type II p38α inhibitors sorafenib[7] and BIRB-796[11] were used as positive controls and were also found to have 3- and 8-fold losses of affinity, respectively. Compound **9** was predicted to be a Type I binder but also showed a 2-fold loss of activity, suggesting that it may stabilize the DFG-out conformation. Interestingly, the K_d values of **3**, **7**, and **8** did not change significantly when measured with active acrylodan-labeled p38α, suggesting that these compounds are in fact weak Type I inhibitors which may not stabilize the DFG-out conformation. It is also possible that these few compounds may interact with acrylodan directly, bind to other sites on the protein, and/or trigger conformational changes which modulate acrylodan fluorescence in the absence of activation loop movement. By traditionally making use of the nonphosphorylated kinase for our binding assay, the sensitivity is increased for the detection of DFG-out binders such as **9** and **16** in HTS screens of large compound libraries, an advantage over traditional activity-based phosphotransfer assays.

(15) Seeliger, M. A.; Nagar, B.; Frank, F.; Cao, X.; Henderson, M. N.; Kuriyan, J. *Structure* **2007**, *15*, 299–311.

Interestingly, compounds **1** and **2** are derivatives of the potent Type I p38α inhibitor SB203580. The detection of these compounds using our novel binding assay served as an internal validation of the results. The binding mode of SB203580 in p38α is well described[6,7] and is unique in that the inhibitor retains a Type I binding mode but is able to bind to and stabilize the DFG-out conformation of p38α by forming $\pi-\pi$ interactions by stacking one of its central planar rings between the side chain of the DFG Phe (Phe169) and the side chain of a Tyr residue (Tyr35) found within the canonical Gly-X-Gly-X-Tyr/Phe-Gly motif of the glycine-rich loop, another highly flexible loop located in the N-terminal lobe of kinases. Given their high affinity and inhibitory activity, **1** and **2** likely adopt a similar binding mode in p38α.

A search in Chemical Abstracts using SciFinder[16] revealed that some of the hit molecules, or related structural analogues, are known for their biological activity on various enzymes but have not yet been linked to kinase inhibition. The biological effects of the tryptamine derivative **5** (Rutaecarpine) have been reviewed recently.[17,18] The naphtholactam **7** binds to p38α with a K_d of ~3 μM, and similar derivatives were designed to conformationally constrain the exocyclic double bond of vinyl-oxindoles which are known to potently inhibit protein kinases.[19] Based on the crystal structure of a trisubstituted naphthostyril in complex with CDK2 (PDB-code: 1p2a), we propose that the lactam carbonyl of **7** interacts with the hinge region of p38α and the trifluoromethyl-benzene moiety binds to the hydrophobic subpocket beyond the gatekeeper residue. The gatekeeper residue is an amino acid situated at the back of the ATP pocket that is well-known for influencing Type I inhibitor affinity and selectivity profiles among kinases.[20] Quinolinones are known kinase inhibitors,[21,22] and binding to the hinge region *via* the lactam moiety is well described (PDB codes: 2hxq, 2i0v). However, N-substituted quinolinones such as **12** and **13** have not previously been described as kinase inhibitors. Attempts to cocrystallize these hits with p38α have so far been unsuccessful. Of particular interest, compounds **9**, **11**, and **16** are not listed in Chemical Abstracts and represent new scaffolds and ligand classes for inhibiting p38α.

3.3. Binding Kinetics and SAR of Selected Hit Compounds. We recently reported the ability of this assay to also detect Type I ligands which utilize the DFG Phe side chain of p38α to stabilize the DFG-out conformation despite adopting a Type I binding mode.[7,23] To gain some insight into the possible binding mode, we performed real-time kinetic measurements of the binding of these compounds to acrylodan-labeled p38α. Type II/III inhibitors are generally characterized as slow binders and often bind with high affinity due to their even slower dissociation rates, whereas Type I inhibitors bind rapidly to the more accessible ATP binding site (regardless of whether they help stabilize the DFG-out conformation).[7,11] Nearly all hits identified in the screen bound rapidly to the kinase ($t_{1/2}$ < 5 s) which suggests a Type I binding mode within the ATP binding pocket. As with SB203580, detection of these ligands suggests that they may also stabilize the DFG-out conformation of the kinase in some manner, thus necessitating further validation in an activity-based inhibition assay. Alternatively, compound **16** and several thiazole-urea compounds (**25**−**31**) bound with significantly slower kinetics which is indicative of binding within the allosteric pocket and the DFG-out conformation of p38α. These thiazole-urea compounds are discussed in greater detail later.

Two hit compounds, **17** and **22**, were limited in amount and not commercially available for testing in an activity-based assay, so several close derivates (**18**−**21**, **23**, **24**) were obtained and screened in addition to all other hits identified in the HTS screen to determine the binding kinetics, K_d, and IC_{50} values for the purpose of studying the SAR of these compounds (Figure 4). Compounds **17**−**24** share a common annelated pyrazine core scaffold but differ in the substitution pattern of the phenyl ring and contain either a cyclohexyl or cyclopentyl ring. Although the binding mode of these compounds is not clear, the limited SAR reveals an essential role of halide substituents in the 4-position of the phenyl ring and the size of the saturated ring system conjugated to the imidazole ring as determinants for compound affinity.

As done for all other hits, acrylodan-labeled p38α was used to perform end point measurements to obtain binding curves for the commercially available derivatives **18**−**20** (Figure 4a). No other derivatives appeared to bind to p38α. In general, we found a clear preference for compounds with a *meta*-substituted phenyl ring, more specifically, with a halogen substituent at this position. Replacement of the *meta*-chlorine of **17** with a *meta*-bromine in **18** resulted in a 100-fold improvement of the K_d. Addition of an *ortho*-hydroxy to the same *meta*-bromo substituted phenyl ring in **19** only slightly reduced the affinity. Furthermore, a comparison of **19** and **22** revealed that replacement of the cyclohexyl with a cyclopentyl ring reduces the affinity of **22** by nearly 10-fold. As was the case with several other hit compounds, **18** and **19** appear to have a much weaker affinity in the activity-based assay, while **20** appeared to have no significant activity. As mentioned for several compounds in Figure 3, the significant reduction of compound activity in the HTRF activity-based assay may be due to the phosphorylation of the activation loop of p38α by MKK6 to activate the kinase, resulting in a decreased likelihood that the kinase will adopt the DFG-out conformation.

To date, cocrystallization of these derivatives with p38α have been unsuccessful and a detailed understanding of the binding mode is not yet possible. However, we could use acrylodan-labeled p38α to gain some insight into the binding mode using real-time kinetic measurements. Upon addition of **18**, we observed a rapid decrease ($t_{1/2}$ < 2 s) in the fluorescence emission of acrylodan at 468 nm (Figure 4b), indicating that this compound, and other detected derivatives (**19** and **20**), are Type I ligands which may somehow induce and stabilize the DFG-out conformation of the kinase. Modeling studies suggest that N1 of the pyrazine ring serves as a hydrogen bond acceptor and interacts with the hinge region of the kinase, while the bromophenyl ring binds into the hydrophobic subpocket and positions the cyclohexyl and cyclopropyl moieties away from the hinge region toward the DFG-motif (*data not shown*).

3.4. Structural Details of Ligand Binding. Kinetic measurements of ligand binding suggested that most compounds were likely to be Type I inhibitors with the exception of **16**, which

(16) Schulz, W. *Chem. Eng. News* **1996**, *74*, 43–44.
(17) Lee, S. H.; Son, J. K.; Jeong, B. S.; Jeong, T. C.; Chang, H. W.; Lee, E. S.; Jahng, Y. *Molecules* **2008**, *13*, 272–300.
(18) Sheu, J.-R. *Cardiovasc. Drug Rev.* **1999**, *17*, 237–245.
(19) Liu, J. J.; Dermatakis, A.; Lukacs, C.; Konzelmann, F.; Chen, Y.; Kammlott, U.; Depinto, W.; Yang, H.; Yin, X.; Schutt, A.; Simcox, M. E.; Luk, K. C. *Bioorg. Med. Chem. Lett.* **2003**, *13*, 2465–8.
(20) Apsel, B.; Blair, J. A.; Gonzalez, B.; Nazif, T. M.; Feldman, M. E.; Aizenstein, B.; Hoffman, R.; Williams, R. L.; Shokat, K. M.; Knight, Z. A. *Nat Chem Biol* **2008**, *4*, 691–9.
(21) Brnardic, E. J.; et al. *Bioorg. Med. Chem. Lett.* **2007**, *17*, 5989–5994.
(22) Peifer, C.; Urich, R.; Schattel, V.; Abadleh, M.; Röttig, M.; Kohlbacher, O.; Laufer, S. *Bioorg. Med. Chem. Lett.* **2008**, *18*, 1431–1435.
(23) Simard, J. R.; Grütter, C. G.; Getlik, M.; Rauh, D. *submitted* 2009.

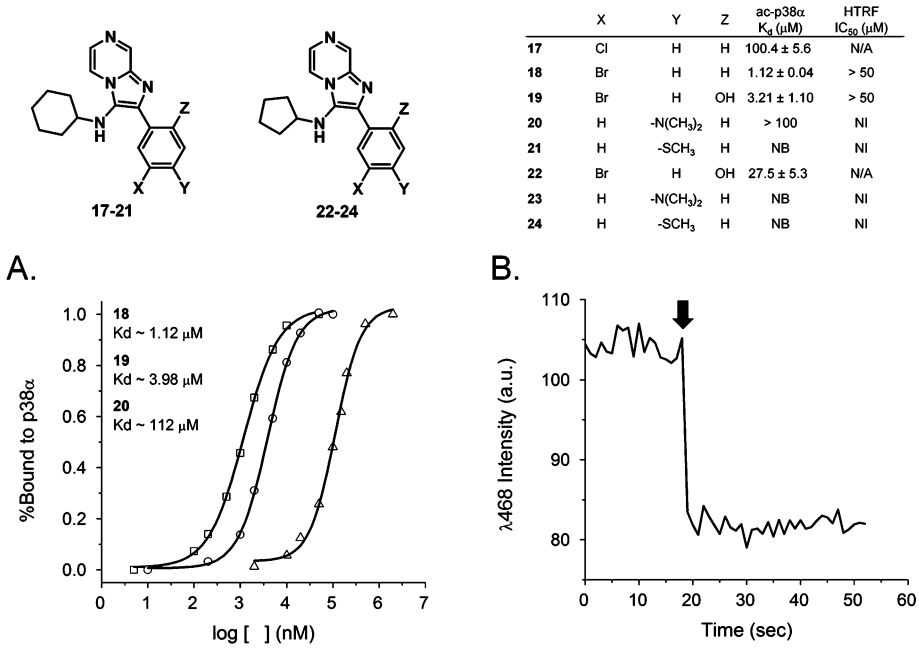

	X	Y	Z	ac-p38α K_d (μM)	HTRF IC_{50} (μM)
17	Cl	H	H	100.4 ± 5.6	N/A
18	Br	H	H	1.12 ± 0.04	> 50
19	Br	H	OH	3.21 ± 1.10	> 50
20	H	$-N(CH_3)_2$	H	> 100	NI
21	H	$-SCH_3$	H	NB	NI
22	Br	H	OH	27.5 ± 5.3	N/A
23	H	$-N(CH_3)_2$	H	NB	NI
24	H	$-SCH_3$	H	NB	NI

Figure 4. SAR and characterization of **17**, **22**, and close derivatives using acrylodan-labeled p38α. Two hits from the HTS screen, **17** and **22**, were not commercially available (N/A) for testing in an activity-based assay. Therefore, several close derivates (**18**−**21**, **23**, **24**) were obtained for IC_{50} determinations and for performing SAR studies on this identified scaffold (top panel). Compounds **21**, **22**, and **24** were not detected by acrylodan-labeled p38α (NB; no binding). Compounds **20**, **21**, **23**, and **24** were not detected in HTRF assay (NI; no inhibition). There was a clear preference for compounds with a *meta*-halogen substituted phenyl ring. As was the case with several other hit compounds, these derivatives have a much weaker effect in the activity-based assay in which the phosphorylated kinase is used. Acrylodan-labeled p38α binding assay was used to determine the K_d of several compounds, including **18** (□), **19** (○), and **20** (△) (B). Real-time kinetic measurements of **18** reveal a rapid decrease ($t_{1/2}$ < 5 s) in the fluorescence emission of acrylodan at 468 nm, indicative of the binding of a Type I ligand (C). The detection of this compound suggests that the compound may promote the DFG-out conformation despite binding primarily within the ATP binding site as observed for other Type I p38α inhibitors.[7] All fluorescence traces and binding curves are representative of at least three independent measurements.

gave a clear slow binding kinetic ($t_{1/2} \approx 38$ s) (Figure S1). This type of slow binding kinetic is characteristic of Type II/III ligands which bind completely or partially within the allosteric pocket of p38α.[7,11] However, the fact that several Type I ligands were sensitively detected in the screen suggests that many of them may somehow stabilize the inactive DFG-out conformation. Compounds similar to **1**, **2**, and **6** are already known as kinase inhibitors which are known to stabilize inactive conformations of p38α or other kinases and for which ample structural information is available. Therefore, we attempted to cocrystallize several of the remaining inhibitors with p38α to obtain detailed structural information about the binding mode and to validate the kinetic information obtained from real-time measurements of ligand binding to acrylodan-labeled p38α (Figure 5) (Table S2). Several compounds either did not cocrystallize with the protein or yielded crystals in which the inhibitor occupancy was too poor to model in the compound properly. Despite these difficulties, we were able to obtain protein X-ray crystal structures of **10**, **14**, **15**, and **25** in complex with p38α. The crystal structure of **25** reveals that the ligand is bound within the allosteric site adjacent to the ATP binding site and that the kinase is in the DFG-out conformation (discussed below) (Figure 6C). This binding mode was in agreement with the slow kinetics of binding observed in our kinetic measurements using acrylodan-labeled p38α.

Interestingly, the remaining structures confirm that the compounds bind in a Type I binding mode, also as predicted by the binding kinetic measurements, but the visible N-terminal end of the activation loop near the DFG motif of p38α is nonetheless found in an inactive conformation (allowing Leu171 to contact each ligand). In the case of **14**, the side chain of Phe169 of the DFG-motif is pointing away from the inhibitor and Leu171 interacts with a hydrophobic patch formed by the indole-substituted inhibitor core (Figure 5F). The inhibitor contains an internal hydrogen bond between the proximal amide bond of the dihydrobenzodioxin and the distal amide bond near the trifluoromethylbenzene moiety and forms a coil within the ATP binding site. This results in the formation of a hydrophobic patch which faces the direction of the Leu171 side chain. Additionally, the inhibitor contains a bulky trifluoromethylbenzene moiety which extends beyond the gatekeeper residue into a hydrophobic subpocket. Moieties occupying this subpocket are known to enhance the potency of ligands for p38α by increasing solvation entropy and may also help shift the conformational equilibrium of p38α such that the DFG-out conformation becomes more energetically favorable. The proximal carbonyl of the inhibitor interacts *via* two hydrogen bonds with the backbone NH of Met109 and Gly110 of the hinge region. The combination of these interactions may also help explain the relatively high affinity of **14** for p38α even when tested for activity against the p38α-dependent phosphorylation of MK2 in a cellular assay (Figure S2). Several derivatives of **14** were also subsequently obtained and tested to investigate the importance of the internal hydrogen bond, as well as other structural features of these ligands, on their affinity for p38α (Figure S3).

Compounds **10** and **15** also bind in a Type I binding mode and contact the hinge region *via* two hydrogen bonds extending between the backbone NH of both Met109 and Gly110 of the

(24) Bukhtiyarova, M.; Karpusas, M.; Northrop, K.; Namboodiri, H. V.; Springman, E. B. *Biochemistry* **2007**, *46*, 5687–96.

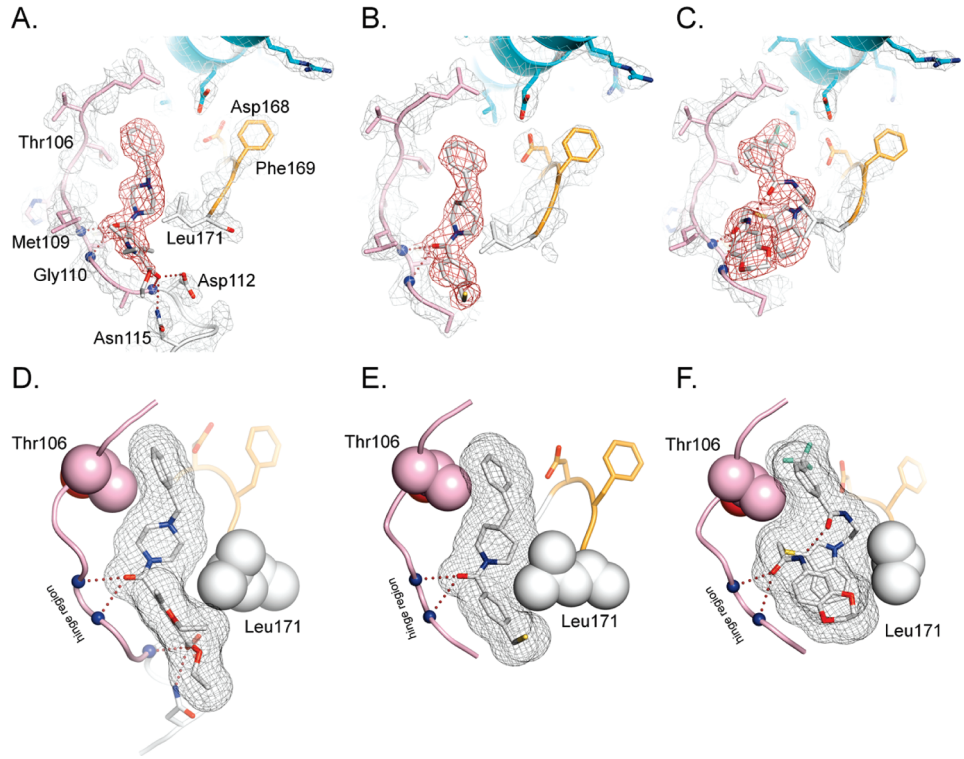

Figure 5. Crystal structures of identified hit compounds **10**, **14**, and **15** bound to p38α. Experimental electron densities (ligand red; protein gray) of the benzylpiperazin-pyrrol **10** (A), the imidazo-pyridine **15** (B), and the indole derivative **14** (C) at 2.1, 2.4, and 2.5 Å resolutions, respectively, are shown ($2F_o - F_c$ map contoured at 1σ). Hydrogen bonding interactions of the inhibitors with the hinge region (colored pink; NH Met 109 and NH Gly110) and the internal hydrogen bond of **14** are shown by red dotted lines. The ethylester of **10** is within hydrogen bonding distance to the backbone (NH Asp112) and side chains (Asp112 and Asn115) of a short helix following the hinge region. The imidazo-pyridine ring of **15** is not visible in the electron density most likely due to structural flexibility in this part of the molecule. In all structures, the kinase domain is found in inactive conformations, and the inhibitors reside in the ATP cleft and approach the hydrophobic subpocket beyond the gatekeeper residue (Thr106). Van der Waals radii of the inhibitors (mesh), the gatekeeper residue, and Phe169 of the DFG-motif (orange) as well as the adjacent Leu171 (white spheres) are shown and depict additional interactions of the inhibitors with the protein which may explain the stabilization of the various inactive conformations (D, E, F). The p38α-**10**, p38α-**14**, and p38α-**15** complexes are in an inactive DFG-"in between" conformation[24] with the side chain of Phe169 pointing away from the hinge region and the inhibitor toward helix C (blue). Most interestingly, in these structures the inactive conformation is stabilized by direct interactions of the inhibitor with the side chain of Leu171.

hinge region and a carbonyl of the inhibitor. Both compounds also share similarities in structure in the vicinity of the gatekeeper (Figure 5D and E) in which a nonplanar six-membered ring is located nearby the side chain of Thr106 of p38α and is connected to a planar phenyl ring by a single carbon atom linker. These two ring moieties overlay nicely in both structures, suggesting that they contribute significantly to the affinity of **10** and **15**. Interestingly, ligands containing diphenyl ether moieties were reported to adopt similar binding geometries around the gatekeeper of p38α,[25] further supporting the argument for the importance of this two ring arrangement to ligand affinity. Similar to **14**, these compounds extend beyond the gatekeeper and penetrate into the hydrophobic subpocket located at the entrance to the allosteric site and may shift the equilibrium toward inactive conformations. Additionally, the kinase was again found to be in the DFG-"in between" conformation which appears to be stabilized by a hydrophobic interaction between Leu171 and each compound.

One can propose that the occupancy of the subpocket beyond the gatekeeper may shift the conformational equilibrium of p38α in the direction of the DFG-out conformation. The most surprising result was that compounds **10**, **14**, and **15** all induced an inactive activation loop conformation while the DFG motif itself appears to be in a DFG-"in between" conformation. This alternate DFG-out conformation has also been reported elsewhere for p38α[24] and is characterized by a significant rearrangement of the activation loop with only partial movement of the Phe169 side chain out of the allosteric site, which it occupies in the DFG-in conformation. In each case, this "in between" conformation appears to be stabilized by a hydrophobic interaction between Leu171 and the surface of each compound. Such a conformational change would also be detected by our assay system. Other possible explanations for these different DFG conformations are discussed further below.

3.5. Novel DFG-Out Binding Mode Identified for Thiazole-Ureas. One of the most interesting findings of this screening initiative was the identification of compounds **25**−**31**, which share a core 2,5-disubstituted thiazole attached to an adjacent urea moiety (Figure 6a). Although the affinity of these compounds is fairly weak (mid μM K_d values), they exhibit similar potency (mid μM IC_{50} values) in inhibiting the activity of phosphorylated p38α kinase. Similar compounds were described previously as Type I Aurora kinase inhibitors.[26] However, these compounds bind to Aurora by forming two hydrogen bonds to the hinge region of the kinase via an N-atom of the urea moiety and the N-atom of the adjacent thiazole ring. Dasatinib is a 2,5-disubstituted thiazole-based Type I inhibitor which inhibits

(25) Michelotti, E. L.; Moffett, K. K.; Nguyen, D.; Kelly, M. J.; Shetty, R.; Chai, X.; Northrop, K.; Namboodiri, V.; Campbell, B.; Flynn, G. A.; Fujimoto, T.; Hollinger, F. P.; Bukhtiyarova, M.; Springman, E. B.; Karpusas, M. *Bioorg. Med. Chem. Lett.* **2005**, *15*, 5274–9.

(26) Andersen, C. B.; Wan, Y.; Chang, J. W.; Riggs, B.; Lee, C.; Liu, Y.; Sessa, F.; Villa, F.; Kwiatkowski, N.; Suzuki, M.; Nallan, L.; Heald, R.; Musacchio, A.; Gray, N. S. *ACS Chem Biol* **2008**, *3*, 180–92.

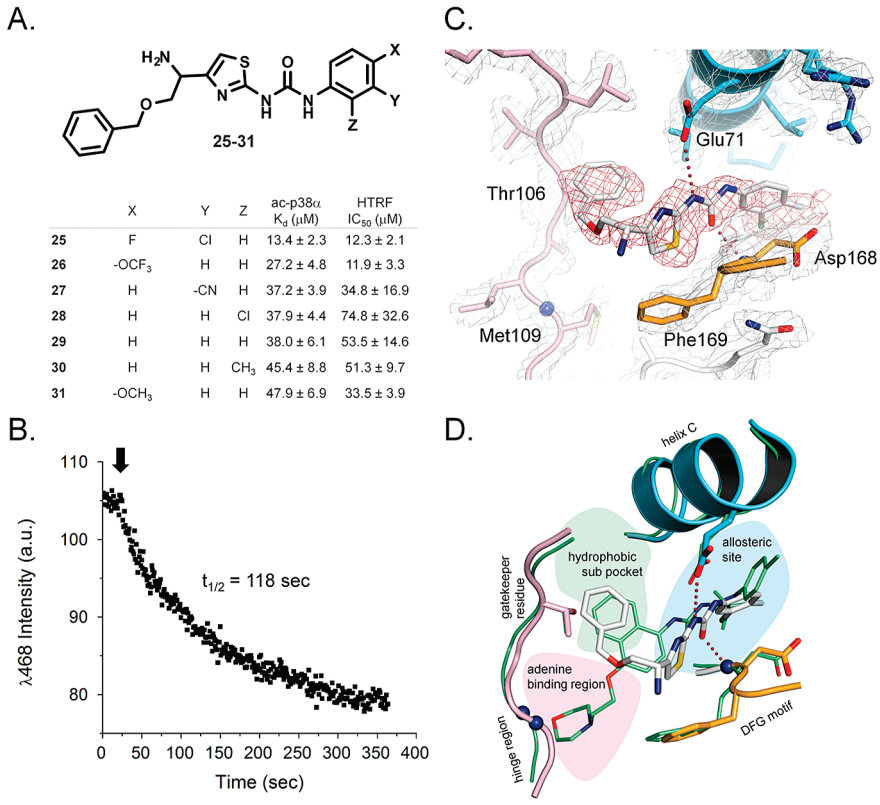

	X	Y	Z	ac-p38α K_d (μM)	HTRF IC_{50} (μM)
25	F	Cl	H	13.4 ± 2.3	12.3 ± 2.1
26	$-OCF_3$	H	H	27.2 ± 4.8	11.9 ± 3.3
27	H	-CN	H	37.2 ± 3.9	34.8 ± 16.9
28	H	H	Cl	37.9 ± 4.4	74.8 ± 32.6
29	H	H	H	38.0 ± 6.1	53.5 ± 14.6
30	H	H	CH_3	45.4 ± 8.8	51.3 ± 9.7
31	$-OCH_3$	H	H	47.9 ± 6.9	33.5 ± 3.9

Figure 6. Characterization of the identified p38α 2,5-disubstituted thiazole-urea inhibitors **25**−**31**. K_d and IC_{50} values determined with the acrylodan-labeled kinase binding assay and the HTRF assay, respectively, are shown along with the general chemical structure of these compounds (A). Upon addition of **25** (black arrow) to a rapidly stirred suspension of acrylodan-labeled p38a, a slow decrease ($t_{1/2}$ = 118 s) in acrylodan fluorescence was observed at 468 nm, indicating slow binding to the DFG-out conformation of p38α (B). All other compounds produced a similar slow binding kinetic (not shown). Cocrystallization of **25** with p38α revealed that the ligand is located completely within the allosteric pocket in a Type III binding mode (C). The phenyl moiety is buried inside the hydrophobic subpocket located beyond the gatekeeper residue. This moiety is conserved in all thiazole-urea compounds identified in the high-throughput screen suggesting it is a crucial contributor to affinity. The urea moiety forms the expected hydrogen bonding interactions with the DFG motif and the side chain of Glu71 of helix C (red dotted lines). The identification of these thiazole-urea compounds as ligands which bind within the allosteric pocket of p38α represents a novel binding mode for this class of compounds. The benzyl moiety of the inhibitor binds into the hydrophobic subpocket flanked by the gatekeeper Thr106 and forces the inhibitor to adopt a constrained conformation when compared to the binding mode of the Type II inhibitor BIRB-796[11] (green thin sticks) (D). The allosteric site, hydrophobic subpocket, and the adenine binding region are color coded. The shown fluorescence trace is representative of at least three independent measurements. All K_d and IC_{50} values represent the mean ± s.d. of at least three independent measurements.

kinases such as cSrc and Abl, lacks a urea moiety, but forms two similar hydrogen bonds with the hinge region, one of which involves the N-atom of the thiazole ring (pdb code: 3g5d for the complex with cSrc and 2zva for the complex with Abl).

To predict the binding mode of **25**−**31**, we used acrylodan-labeled p38α to measure the binding kinetics in real-time (Figure 6b). In the case of **25**, the binding rate was very slow ($t_{1/2}$ = 118 s), and as in the case of **16** described above, this kinetic data suggested that these thiazole-ureas adopt a previously unreported novel binding mode by slowly binding to the DFG-out conformation of p38α. All other thiazole-urea hit compounds behaved similarly (*data not shown*).

To confirm and validate these predictions, we cocrystallized **25** with wild type p38α (Figure 6c) (Table S2). As predicted, the ligand is located exclusively within the allosteric pocket of the DFG-out conformation. Surprisingly, the crystal structure revealed that a phenyl moiety which is tethered to the central thiazole ring via a flexible linker folds back on itself and becomes buried inside the hydrophobic subpocket located beyond the gatekeeper residue. This moiety is conserved in all thiazole-urea compounds identified in this screening initiative, suggesting that it is a crucial contributor to the affinity of **25**−**31**. Additionally, the urea moiety formed the expected interactions with the backbone NH of Asp168 of the DFG-motif and Glu71 of the C-helix, and these interactions may be stabilized by the binding of the before mentioned phenyl ring into the hydrophobic subpocket. At the same time, the conformational strain introduced by the folding of this moiety into the subpocket may cause the plane of the thiazole-urea portion of the ligand to shift when compared to BIRB-796 (Figure 6D). Ironically, the conserved moiety which may enable these compounds to bind as Type III inhibitors with a high enough affinity to be detected may also be the reason for which the urea moiety cannot attain the optimal geometry for forming stronger hydrogen bonds. Future chemistry endeavors are currently underway to investigate these issues.

4. Discussion

Identification of hit molecules which can be developed into promising new lead compounds is mainly driven by the screening of large compound collections, where up to millions of chemical entities form a single compound library. These large screening campaigns are often very costly, the odds of identifying new scaffolds is very low, and such screens represent only the initial phase of drug discovery. In the case of anticancer drugs, which often target kinases, the discovery of innovative new drugs is becoming increasingly hampered (i.e., ∼50% fail

to be approved) by rising R&D costs and lower success rates in the most expensive phase of clinical trials (Phase III) compared to other drugs.[27] This is due largely in part to limited target specificity, one of the major roadblocks which currently plague kinase research efforts. The most recent success stories in targeted cancer therapy are the newest approved anticancer drugs such as sorafenib (Nexavar; Bayer), nilotinib (Tasigna; Novartis), sunitinib (Sutent; Pfizer/Sugen), dasatinib (Sprycel; Bristol Myers Squibb), and lapatinib (Tykerb; GlaxoSmithKline) which target specific types of cancer.[27] The key to their success is that many of these more "Modern" drugs adopt alternative binding modes and take advantage of inactive kinase conformations. Ironically, the onset of these high profile anticancer agents has also brought the problem of mutation-associated drug resistance to the forefront, calling for new possibilities to develop new generations of kinase inhibitors which can circumvent drug resistance in effected patients.

Since classical kinase activity assays rely on the kinase to be phosphorylated and in the active conformation, its ability to adopt the inactive conformation is reduced, resulting in an enrichment of hits of Type I scaffolds and desensitization to weaker DFG-out binders. A high number of known Type I kinase inhibitors are more sensitive to drug resistance and limited selectivity, which may be a direct consequence of their discovery using standard enzymatic assays to screen large compound libraries.[7] In response to current medicinal chemistry and chemical biology endeavors to identify and develop inhibitors that target alternative binding sites and stabilize inactive kinase conformations,[1,28−31] we recently developed FLiK as a novel direct binding assay for p38α and other protein kinases. This system takes advantage of conformational changes in the kinase domain triggered by ligand binding and can specifically identify and enrich for compounds which stabilize the inactive kinase conformation and may unlock the full potential of pre-existing inhibitor libraries. The approach was also extended to the tyrosine kinase cSrc,[8] highlighting wider application to both major kinase families and the benefit of screening using the unphosphorylated kinase to detect weak DFG-out binders. These findings were then subsequently used to address gatekeeper mutation-associated drug resistance via structure-based drug design.[9]

Here we present the successful application of this assay system to screen a larger compound library (~35000 compounds) in high-throughput. We identified several compounds which stabilized the inactive DFG-out conformation of p38α and validated these hits in an activity-based assay system and solved the protein X-ray crystal structures of several compounds in complex with the target kinase. These studies allowed us to gain insight into the ligand binding mode as well as a better understanding of how some ligands may promote and stabilize the DFG-out conformation of p38α. Among these compounds, we identified DFG-out binding thiazole-urea compounds as weak inhibitors of p38α. These compounds adopt a Type III binding mode, a new binding mode for this widely used scaffold, and bind exclusively within the allosteric pocket adjacent to the ATP binding site. These results will stimulate further medicinal chemistry efforts to improve the affinity of this compound class for the DFG-out conformation.

In contrast to these thiazole-ureas and **16**, most of the identified inhibitors appear to be Type I compounds which bind in the ATP binding site and contact the hinge region of the kinase. We have previously shown that this direct binding assay system can sensitively detect some Type I ligands which adopt unique binding modes and, in doing so, can stabilize the DFG-out conformation of p38α.[7,23] The movement of the activation loop which accompanies the conformational change directly changes the environment of the attached fluorophore, thereby allowing these compounds to be detected. The crystal structures obtained for some of the identified hits reveal several unique Type I inhibitors which do not extend into the allosteric site but appear to modulate the conformation of the DFG-motif and/or activation loop by directly interacting with amino acids past the DFG-motif.

In the case of **10**, **14**, and **15**, the side chain of Leu171 (DFG+1) migrates deep into the ATP binding site to interact with a hydrophobic surface on the compounds. In **14**, this enlarged surface is created by the formation of an internal hydrogen bond and a unique "folding" of the inhibitor in the ATP binding site. These extra interactions may help destabilize the DFG-in conformation and, in the case of **14**, explain the particularly high affinity of this ligand for p38α. Alternatively, the explanations are less clear in the case of compound **15**, which shares very similar chemical moieties when compared to **10**. These moieties bind in a conserved geometry around the gatekeeper residue such that the terminal planar phenyl ring is buried within the hydrophobic subpocket at the entrance to the allosteric site. The crystal structures of compounds **10**, **14**, and **15** reveal a DFG-"in between" conformation where the DFG Phe side chain does not appear to contact the inhibitor, but visible segments of the N-terminal portion of the activation loop are clearly reoriented, thereby explaining the detection of these compounds. We propose that the binding of bulky moieties in the hydrophobic subpocket behind the gatekeeper may somehow result in a more energetically favored DFG-out conformation since this subpocket is occupied in the case of all three Type I inhibitor structures presented in Figure 5.

Compounds similar to **10** and **15** were previously reported as binding to the DFG-in conformation. Of note, one particular subset of these compounds induced a change in the glycine rich-loop (also known as P-loop) conformation such that Tyr35, which is located within the canonical Gly-X-Gly-X-Tyr/Phe-Gly motif of p38α, is pulled under the glycine-rich loop and stacks against the inhibitor. The glycine-rich loop is another highly flexible structural element conserved among all ATP/GTP binding proteins[32] and is located in the N-terminal lobe of kinase domains and serves as a regulatory "flap" controlling the entry of ligands and substrates into the ATP binding site.[33] This feature helps to shield ATP and some Type I inhibitors in the ATP binding pocket from the surrounding solvent[34−36] and helps augment ligand affinities.

(27) DiMasi, J. A.; Grabowski, H. G. *J Clin Oncol* **2007**, *25*, 209–16.
(28) Adrian, F. J.; Ding, Q.; Sim, T.; Velentza, A.; Sloan, C.; Liu, Y.; Zhang, G.; Hur, W.; Ding, S.; Manley, P.; Mestan, J.; Fabbro, D.; Gray, N. S. *Nat Chem Biol* **2006**, *2*, 95–102.
(29) Calleja, V.; Laguerre, M.; Parker, P. J.; Larijani, B. *PLoS Biol* **2009**, *7*, 189–200.
(30) Fischmann, T.; Smith, C.; Mayhood, T.; Myers, J.; Reichert, P.; Mannarino, A.; Carr, D.; Zhu, H.; Wong, J.; Yang, R. S.; Le, H.; Madison, V. *Biochemistry* 2009. doi:10.1021/bi801898e.
(31) Kirkland, L. O.; McInnes, C. *Biochem. Pharmacol.* **2009**, *77*, 1561–71.
(32) Saraste, M.; Sibbald, P. R.; Wittinghofer, A. *Trends Biochem. Sci.* **1990**, *15*, 430–4.
(33) Tamayo, N.; Liao, L.; Goldberg, M.; Powers, D.; Tudor, Y. Y.; Yu, V.; Wong, L. M.; Henkle, B.; Middleton, S.; Syed, R.; Harvey, T.; Jang, G.; Hungate, R.; Dominguez, C. *Bioorg. Med. Chem. Lett.* **2005**, *15*, 2409–13.
(34) Hanks, S. K.; Hunter, T. *FASEB J* **1995**, *9*, 576–96.

Since there is some cross-talk between the glycine-rich loop, the DFG motif, and the activation loop, we also propose a role for the glycine-rich loop in mediating the interplay between DFG-in and DFG-out in p38α. It is believed that these two loops interact with one another through the formation of a hydrophobic interface in some kinases, thereby allowing the glycine-rich loop to modulate the conformational equilibrium of the kinase to favor the inactive DFG-out conformation.[37] Mutations in either loop, which frequently occur in various cancers,[37] disrupt this patch and favor the more active DFG-in conformation. Therefore, we believe that the different binding modes observed for **10**, **15**, and previously published compounds may be explained by variations in the glycine-rich loop conformation. Depending on the structure of the ligand, planar side chains of highly conserved Tyr or Phe residues in the glycine-rich loop may interact directly with the ligand and pull the loop down into the ATP binding site. Such an interaction would likely keep the kinase activation loop in its open, extended conformation (DFG-in). If the glycine-rich loop is upward and extended, this may promote the closed activation loop conformation (DFG-out). In this case, the side chain of the DFG Phe may provide the more favorable interaction to stabilize ligand binding. The structure of the ligand may also dictate which of these loops plays a role in directly stabilizing the bound ligand, highlighting a dynamic interplay of these two regulatory loops with ligands bound within the catalytic cleft.

5. Conclusions

By providing an innovative new method to differentiate between inhibitors which bind to the DFG-out conformation in high throughput, we provide proof that new types of molecules can be identified in already existing compound libraries using FLiK and we show that some of these hits were not detected in classical kinase assays, further indicating the bias of FLiK for identifying compounds based on the activation state of the target kinase. The key is that the assay can be used to screen for ligand binding by facilitating unphosphorylated, inactive forms of the target kinase and in the absence of competing ligands such as ATP which is often present in mM concentrations in traditional screening assays. This may in fact heighten the sensitivity to ligands which bind weakly to the allosteric pocket and/or Type I inhibitors which stabilize the DFG-out conformation. Such compounds might otherwise be missed in traditional assay setups. We propose that the here described screening setup will also prove valuable in high-throughput prescreening of fragment libraries prior to cocrystallization or soaking experiments to assist early stages of fragment-based design approaches. Ongoing medicinal chemistry studies will further prove if the hit compounds identified here can be further developed into potent and selective kinase inhibitors.

Acknowledgment. We thank Sigrid Rosin-Steiner for her expertise and assistance with pipetting the screen and Willem van Otterlo for helpful discussions. We also thank Slava Ziegler, Franziska Thorwirth, Piotr Liguzinski, and Jan Eickoff for helpful discussions regarding the cellular assay. JRS was funded by the Alexander von Humboldt Foundation. This work was supported by the German Federal Ministry for Education and Research through the German National Genome Research Network-Plus (NGFN-Plus) (Grant No. BMBF 01GS08102). Schering-Plough, Bayer-Schering Pharma, Merck-Serono and Bayer CropScience are thanked for financial support.

Supporting Information Available: All crystal structures described in this manuscript were deposited into the Protein Data Bank (PDB codes: 3iw5, 3iw6, 3iw7, and 3iw8). Experimental details for the data collection and refinement statistics for p38α cocrystallized with several ligands, additional figures, complete ref 21, as well as further discussions regarding the SAR of additional inhibitors. This material is available free of charge via the Internet at http://pubs.acs.org.

JA907795Q

(35) Mapelli, M.; Massimiliano, L.; Crovace, C.; Seeliger, M. A.; Tsai, L. H.; Meijer, L.; Musacchio, A. *J. Med. Chem.* **2005**, *48*, 671–9.
(36) Patel, S. B.; Cameron, P. M.; O'Keefe, S. J.; Frantz-Wattley, B.; Thompson, J.; O'Neill, E. A.; Tennis, T.; Liu, L.; Becker, J. W.; Scapin, G. *Acta Crystallogr D Biol Crystallogr* **2009**, *65*, 777–85.
(37) Wan, P. T.; Garnett, M. J.; Roe, S. M.; Lee, S.; Niculescu-Duvaz, D.; Good, V. M.; Jones, C. M.; Marshall, C. J.; Springer, C. J.; Barford, D.; Marais, R. *Cell* **2004**, *116*, 855–67.